



RESEARCH ARTICLE

WILEY

Improvement of a simplified process-based model for estimating transpiration under water-limited conditions

Na Liu^{1,2} | Thomas N. Buckley³ | Xinguang He^{1,4} | Xinping Zhang^{1,4} |
Cicheng Zhang¹ | Zidong Luo^{1,2} | Hailong Wang² | Nasrin Sterling² | Huade Guan²

¹College of Resource and Environmental Science, Hunan Normal University, Changsha, China

²National Centre for Groundwater Research and Training, College of Science and Engineering, Flinders University, Adelaide, South Australia, Australia

³Department of Plant Sciences, University of California, Davis, Davis, California, USA

⁴Key Laboratory of Geospatial Big Data Mining and Application, Hunan Normal University, Changsha, China

Correspondence

Xinguang He, College of Resource and Environmental Science, Hunan Normal University, Changsha 410081, China.
Email: xghe@hunnu.edu.cn

Huade Guan, National Centre for Groundwater Research and Training, College of Science and Engineering, Flinders University, Adelaide, SA 5001, Australia.
Email: huade.guan@flinders.edu.au

Funding information

China Scholarship Council; National Centre for Groundwater Research and Training, Australian Research Council, Grant/Award Number: SR08000001; USDA National Institute of Food and Agriculture, Grant/Award Number: 1016439; Grains Research and Development Corporation, Grant/Award Number: US00082; International Wheat Yield Partnership, Grant/Award Number: IWYP89; National Science Foundation, Grant/Award Number: 1557906; Hunan Provincial Innovation Foundation for Postgraduate, Grant/Award Number: CX2017B181; Hunan Bairen Program, Grant/Award Number: 2012001; Construct Program of Key Discipline in Hunan Province of China, Grant/Award Number: 2011001; National Natural Science Foundation of China, Grant/Award Numbers: 41571021 and 41472238

Abstract

Plant transpiration depends on environmental conditions, and soil water availability is its primary control under water deficit conditions. In this study, we improve a simplified process-based model (hereafter “BTA”) by including soil water potential (ψ_{soil}) to explicitly represent the dependence of plant transpiration on root-zone moisture conditions. The improved model is denoted as the BTA- ψ model. We assessed the performance of the BTA and BTA- ψ models in a subtropical monsoon climate and a Mediterranean climate with different levels of water stress. The BTA model performed reasonably in estimating daily and hourly transpiration under sufficient water conditions, but it failed during dry periods. Overall, the BTA- ψ model provided a significant improvement for estimating transpiration under a wide range of soil moisture conditions. Although both models could estimate transpiration (sap flow) at night, BTA- ψ was superior to BTA in this regard. Species differences in the calibrated parameters of both models were consistent with leaf-level photosynthetic measurements on each species, as expected given the physiological basis of these parameters. With a simplified representation of physiological regulation and reasonable performance across a range of soil moisture conditions, the BTA- ψ model provides a useful alternative to purely empirical models for modelling transpiration.

KEYWORDS

environmental variables, soil water deficit, transpiration estimation

1 | INTRODUCTION

Transpiration (E_c) plays an important role in land-surface energy and water balance, amounting to roughly 40% of terrestrial precipitation (Oki & Kanae, 2006; Schlesinger & Jasechko, 2014) and influencing regional and global climate (Dickinson, 1987; Fatichi, Pappas, & Ivanov, 2016; LeMone et al., 2007). Transpiration depends on environmental conditions and will respond to changes in climate and local hydrological conditions (Gharbia, Smullen, Gill, Johnston, & Pilla, 2018). Accurate estimation of transpiration is therefore crucial to understanding how hydrometeorological conditions (e.g., solar radiation, soil water status, temperature, vapour pressure deficit, and CO_2 concentration) impact plant function, drought response, and mechanisms of mortality (e.g., hydraulic failure and carbon starvation; Hartmann, Ziegler, Kolle, & Trumbore, 2013; McDowell et al., 2008).

A number of approaches have been developed for estimating transpiration. Because transpiration is coupled with photosynthesis (Cowan, 1982), many models use the coupling of net CO_2 assimilation rate (A_n) and stomatal conductance (g_s) to constrain models of plant-atmosphere CO_2 and water vapour exchange (Best et al., 2011; Boussetta et al., 2013; Oleson et al., 2010). Nevertheless, it is often desirable to estimate transpiration independently from photosynthesis. For example, one of the two transpiration models adopted in the Noah land surface model estimates transpiration based on the Jarvis scheme (Wei, Xia, Mitchell, & Ek, 2013). The enhanced Physiological Principles in Predicting Growth (3PG+) forest growth model integrated into the Catchment Analysis Tool (Beverly, Bari, Christy, Hocking, & Smettem, 2005) adopted the Food and Agriculture Organization approach based on potential evapotranspiration (Feikema et al., 2010). AquaCrop, a crop water productivity model developed by the Land and Water Division of Food and Agriculture Organization, mainly focuses on water dynamics and balance (Saccon, 2018), in which transpiration is estimated from the crop coefficient and reference evapotranspiration (ET_0 ; Allen, Pereira, Raes, & Smith, 1998).

Several methods are available to estimate E_c independent of photosynthesis. The Penman–Monteith (P-M) equation is one of the most widely used methods for estimating plant water use (Khamzina, Sommer, Jpa, & Plg, 2009; Pereira, Green, & Nova, 2006). A few other models estimate E_c directly by calculating a theoretical maximum transpiration rate and then reducing actual transpiration below this maximum using stress functions based on environmental inputs (Mission, Panek, & Goldstein, 2004; White, Beadle, Sands, Worledge, & Honeysett, 1999; Whitley, Medlyn, Zeppel, Macinnis-Ng, & Eamus, 2009); this method is often referred to as the modified Jarvis–Stewart method (MJS), as the stress functions are formulated in a manner similar to the Jarvis–Stewart approach (Jarvis, 1976; Stewart, 1988). MJS requires fewer parameters and input variables than the P-M equation, and it calculates transpiration directly from environmental variables, bypassing canopy conductance (g_c).

Process-based models have also been developed to estimate transpiration rates (Choudhury & Digirolamo, 1998; Federer, 1979; Gao, Zhao, Zeng, Cai, & Shen, 2002). These models include

parameters that explicitly represent measurable biophysical properties or traits, for example, leaf-specific hydraulic conductance, soil water potential or leaf water potential, and epidermal osmotic pressure. Because direct quantification of these traits is often time-consuming and requires specialized equipment, process-based models for tree water use are perceived to have limited applicability for catchment managers (Gharun, Turnbull, Henry, & Adams, 2015). Buckley, Mott, and Farquhar (2003) proposed a process-based model (hereafter BMF) based on biophysical process laws for gas exchange and water transport and experimentally supported hypotheses about how stomata respond to leaf water potential. Rodriguez-Dominguez et al. (2016) used a modified version of the BMF model to clarify the mechanisms of stomatal regulation under soil drought. Buckley, Turnbull, and Adams (2012) simplified the BMF model in another form, which is now referred to as the “BTA” model (Wang, Guan, & Simmons, 2016). The BTA model, which includes just two environmental variables (incoming shortwave radiation and vapour pressure deficit), was able to simulate sap flux and stomatal conductance for two south-east Australian species at different time scales (Buckley et al., 2012). Xu, Yu, Ji, and Studicky (2017) have shown that the BTA model outperforms the MJS model in arid regions. Wang et al. (2016) demonstrated that the MJS and BTA models generally outperform the P-M equation for simulating tree water use under Mediterranean-type climate conditions.

When the original process-based model (Buckley et al., 2003) was simplified by Buckley et al. (2012), three biophysical parameters—the leaf-specific plant hydraulic conductance, K_l ; the leaf solute potential, $\psi_{s,\text{leaf}}$; and the soil water potential, ψ_{soil} —were combined into a single parameter intended to be estimated empirically, $E_{\text{max}} = K_l (\psi_{\text{soil}} - \psi_{s,\text{leaf}})$. One rationale for this simplification was that, in many species, osmotic adjustment (active decline in $\psi_{s,\text{leaf}}$ by solute accumulation in leaves) counterbalances declining soil water potential, such that E_{max} remains approximately constant, obviating the need to measure its component parameters directly. As a result, the BTA model does not explicitly include soil moisture. However, Wang et al. (2016) reported that BTA fails to simulate transpiration accurately when soil water condition varies widely. We hypothesized that this failure could be remedied, and the model's performance under varying soil moisture conditions could be improved, by expanding the parameter E_{max} to reflect its dependence on soil water potential. We refer to the BTA model with expanded E_{max} function as the “BTA- ψ ” model.

Another benefit of process-based models is their ability to inform understanding of the physiological basis of observed variations in tree growth, water use, and environmental responses (Houghton, Jenkins, & Ephraums, 1990). Despite the BTA model's simplifications, its parameters nevertheless bear transparent relationships to the underlying biophysical parameters, so the model remains potentially useful in this respect (Buckley et al., 2012; Wang et al., 2016). Buckley et al. (2012) demonstrated this for two eucalypt species. However, the BTA model's ability to provide insights about the processes underlying transpiration has not been explored further, and this has not been examined at all for the BTA- ψ .

The objectives of this study were (a) to improve the performance of the BTA model in estimating transpiration across a wide range of water conditions by making the role of soil water potential explicit, as in the original BMF model, and (b) to assess the capability of the BTA and BTA- ψ models to infer physiological processes by comparing their calibrated parameters with values derived from leaf-level gas exchange measurements. We examined the performance of both models across four species in two climate zones, at both daily and hourly scales.

2 | METHODOLOGY

2.1 | Sites and target species

The experiments in this study were conducted at three sites. The first was near the campus of Flinders University (138°34'28"E, 35°01'49" S, elevation 100 m) in Adelaide, South Australia. The climate of Adelaide is Mediterranean, characterized by hot and dry summers and mild and rainy winters. Two *Allocasuarina verticillata* trees, a typical conifer in South Australia, were selected as the target species in this study. The measurements for *A. verticillata* were performed over two periods: January to April and October to December in 2012.

The other two sites were in Wangjiawan (112°53'20"E, 28°09'46" N, elevation of 70 m) and the Yuelu Mountain (112°55'58"E, 28°10'34"N, elevation 195 m), both located in Changsha, the capital city of Hunan Province in the central south of China. The sites are away from dense residential areas. The study areas have a subtropical monsoon climate characterized with hot and wet summers and cold and dry winters. Precipitation is concentrated in spring and early summer, followed by a dry period in July and August (Liu, Guan, Luo, et al., 2017). Two individuals of *Osmmanthus fragrans* and one of *Cinnamomum camphora* were monitored in Wangjiawan during the growing season (from April to September) in 2013. Both species are evergreen trees, widely distributed in southern China. Data after August 1, 2013, were excluded for *C. camphora* due to drought-induced leaf senescence. Another *C. camphora* and two *Liquidambar formosana* trees were measured in Yuelu Mountain from 2014 to 2015. *L. formosana* is a common local deciduous species, whose leaves appear in spring and fall in

autumn. All experimental trees were mature individuals. Data about the study sites and trees are summarized in Table 1.

2.2 | Field measurements

2.2.1 | Measurement of micrometeorological data

Micrometeorological data were collected from a standard automatic weather station (WeatherHark-232, USA), which was installed on a flat piece of open land in each experimental site, with a distance from target trees in a range of 20–50 m. Wind speed, relative humidity, air temperature, precipitation, and solar radiation were measured. Measurement frequency of the automatic weather stations was set at a 15-min interval in Adelaide and a 30-min interval in Changsha. Subhourly data were averaged for air temperature, relative humidity, and wind speed and summed for solar radiation and precipitation to hourly and daily values. There was a month-long drought period (from July to August) in the summer of 2013 in Changsha. Total precipitation from July to August in 2013 was about 32% of the average for the same period from 1982 to 2013. In Adelaide, episodic rain events during dry summer and autumn regularly produce a wide range of moisture conditions. These variations in soil moisture provide a good opportunity to examine the performance of the BTA and BTA- ψ models under progressive soil drying. The temporal variation of meteorological measurement at the two studied zones is shown in Figure 1.

2.2.2 | Measurement of sap flow

Sap flow was measured with heat-pulse sap flow sensors (SFM, ICT International Pty Ltd, Australia) at 30-min intervals. For each tree, two sets of sap flow probes were installed in the south and north sides of the trunk, at a height of 1.3 m above ground. A software "sap flow tool" from the provider was used to calculate the daily and hourly sap flow rates, with input observed parameters including sapwood depth, bark thickness, sapwood fresh and dry weight, and sapwood fresh volume, based on the method described in Burgess et al. (2001). The sap flow rates were estimated from the average values of the two sets of probes installed in each tree.

TABLE 1 Selected information for tree of the four species used in this study

Target tree	Site	Period of data record	Plant type	Tree age (years)	DBH (cm)	Height (m)	L_c (m ² m ⁻²)
<i>Allocasuarina verticillata</i> 1	Flinders	Jan. to Apr. and Oct. to Dec. 2012	Conifer		15	6	1.9
<i>A. verticillata</i> 2	Flinders	Oct. to Dec. 2012	Conifer		13	6	1.8
<i>Osmmanthus fragrans</i> 1	Wangjiawan	Apr. to Sep. 2013	EB	10	7.6	4.5	4.3
<i>O. fragrans</i> 2	Wangjiawan	Apr. to Sep. 2013	EB	10	8.7	3.8	4.3
<i>Cinnamomum camphora</i> 1	Wangjiawan	Apr. to Jul. 2013	EB	8	15.8	6.0	1.8
<i>C. camphora</i> 2	Yuelu Mountain	Apr. 2014 to Nov. 2015	EB	12	19.1	8.1	3.1
<i>Liquidambar formosana</i> 1	Yuelu Mountain	Apr. 2014 to Nov. 2015	DB	50	39.8	17.2	3.6
<i>L. formosana</i> 2	Yuelu Mountain	Jun. to Oct. 2015	DB	40	35.0	17	3.4

Note. DBH: tree diameters at breast height; EB: evergreen broad-leaved; DB: deciduous broad-leaved; L_c : canopy leaf area index.

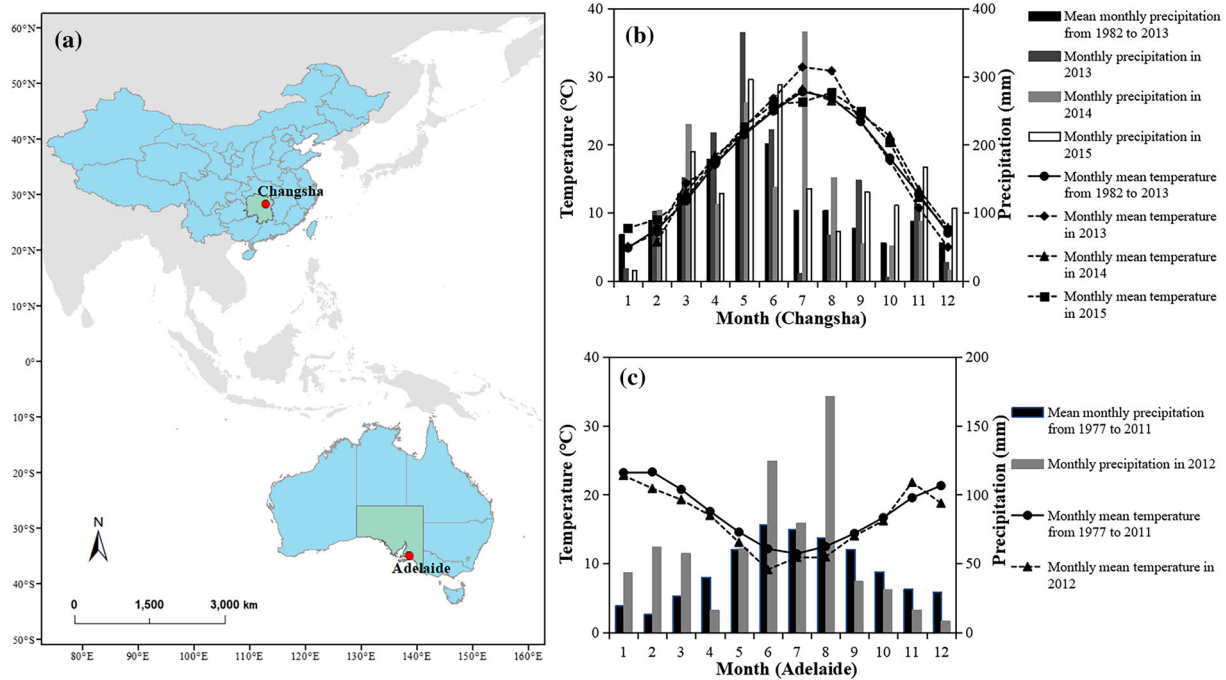


FIGURE 1 Map (a) and climatic characteristics (b and c) of the experiment sites. Monthly mean temperature (lines) and mean monthly precipitation (bars) and the measured values over the experiment period in Changsha (b) and Adelaide (c). A severe drought occurred in July 2013 and heavy precipitation occurred in summer 2014 and 2015 in Changsha. Meteorological data from 1982 to 2013 in Changsha are from the National Meteorological Information Center (<http://data.cma.cn/>), and data from 1977 to 2011 in Adelaide are from the Bureau of Meteorology (<http://www.bom.gov.au/>)

2.2.3 | Measurement of predawn leaf water potential

The predawn leaf water potential was measured using a Scholander-type pressure chamber (PMS 1000, PMS Inst., Corvallis, OR, USA) between 5:00 a.m. and 6:00 a.m., once weekly from June to September in 2013 at the site in southern China. Two branches with healthy leaves were cut off from the target tree, and the water potential of one leaf from each branch was measured using the PMS. If the two observed values differed by less than 0.2 MPa, their averaged value was the final predawn leaf water potential for this tree at that day. If the error was over 0.2 MPa, two more branches were selected to measure the leaf water potential, and then all measured values of this tree were averaged as the final value.

2.2.4 | Measurement of predawn stem water potential

Stem water potential was measured every 30 min with thermocouple stem psychrometers (PSY1, ICT International Pty Ltd, Australia), developed by Dixon and Tyree (1984). Water potential along the soil-root-stem-leaf continuum is commonly assumed to be in equilibrium at predawn (Wang, Guan, Deng, & Simmons, 2014; Yang et al., 2013), and our data support this assumption (e.g., Figure 2a). Therefore, in this study, we used predawn stem water potential (averaged between 4:00 a.m. and 6:00 a.m.) as a surrogate for root-zone soil water potential. Figure 2a,b shows how stem water potential varied over time in *O. fragrans* 1 and *A. verticillata* 1.

2.2.5 | Measurement of canopy leaf area index

Digital cover photography (Pekin & Macfarlane, 2009) was adopted to calculate canopy leaf area index (L_c) in this study. The method uses vertical field-of-view canopy pictures taken by cameras and then calculates L_c in Matlab using code written by Pekin and Macfarlane (2009).

2.2.6 | Measurement of leaf gas exchange

Leaf-level gas exchange was measured using an Li-6400 portable photosynthesis system (LI-COR, USA). Photosynthetically active radiation (PAR) was provided by a red/blue light source (LI-6400-02B) connected to the system with photosynthetic photon flux density varying between 0 and 2,000 $\mu\text{mol m}^{-2} \text{s}^{-1}$. Light response curves were measured on sunny days; more details can be found in Luo, Guan, Zhang, and Liu (2017). For broad-leaf species, the one-sided leaf area included in the leaf chamber was input to calculate net photosynthesis rates, whereas for needle-leaf species, the total leaf surface area was used, as leaves in the chamber were exposed to light from all directions.

2.3 | Upscaling sap flow to canopy transpiration

Transpiration rates were calculated from sap flow measurements based on the equation (Yang et al., 2013):

$$E_c = \frac{Q}{A_c}, \quad (1)$$

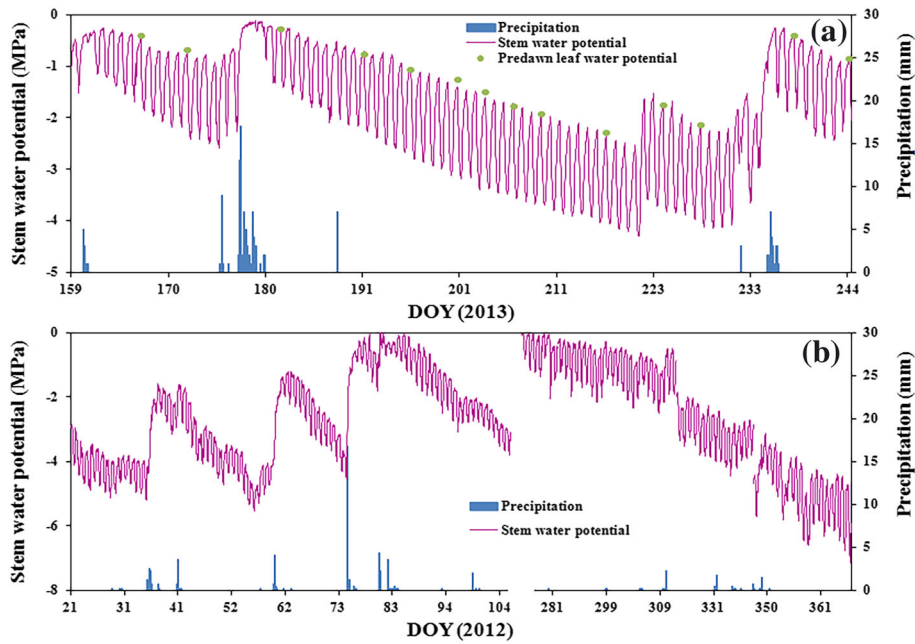


FIGURE 2 (a) Half-hourly stem water potential and predawn leaf water potential of *Osmmanthus fragrans* 1, and precipitation from June to September (from DOY 159 to 244) in 2013. The difference between predawn leaf and stem water potential is minor, indicating water potential equilibrium within the plant at predawn. Stem water potential increased at DOY 221 because of irrigation. (b) Half-hourly stem water potential of *Allocasuarina verticillata* 1, and precipitation during two measured periods (from DOY 21 to 106 and DOY 275 to 366) in 2012. DOY is the day of the year (i.e., 1 = January 1)

where A_c is the effective canopy leaf area (cm^2) and Q is the volumetric sap flux ($\text{cm}^3 \text{ day}^{-1}$ or $\text{cm}^3 \text{ hr}^{-1}$). The effective canopy area is required to convert volumetric sap fluxes (on a sapwood area basis; i.e., $\text{cm}^3 \text{ water} \cdot \text{cm}^{-2} \text{ sapwood} \cdot \text{hr}^{-1}$) to transpiration rates (on a ground area basis; i.e., $\text{cm}^3 \text{ water} \cdot \text{cm}^{-2} \text{ ground} \cdot \text{hr}^{-1}$). A_c conceptually is not necessarily the projected canopy area, as it is related to canopy leaf area index, root distribution of specific sample trees, as well as soil properties.

With an assumption that A_c does not change with season for evergreen species (*A. verticillata*, *O. fragrans* and *C. camphora*), and within the growing season of the deciduous species (*L. formosana*), A_c can then be estimated by matching E_c to potential transpiration during the days with optimal soil moisture, for example, in a sunny day following a sizable rainfall. We adopt a hybrid dual source model (Guan & Wilson, 2009) to estimate potential transpiration of a tree.

2.4 | Leaf-level photosynthesis data analysis

Canopy transpiration is connected to leaf-level stomatal responses, which can be measured by leaf gas exchange. Thus, we compared parameters derived at the canopy level from the BTA and BTA- ψ models against those from leaf-level gas exchange measurements. Leaf-level photosynthesis light responses (i.e., the response of photosynthesis to irradiance) for each species were fitted to a nonrectangular hyperbola (Cernusak, Hutley, Beringer, Jam, & Turner, 2011; Johnson & Thornley, 1984; Marshall & Biscoe, 1980):

$$A = \frac{\Phi I + A_{\max} - \sqrt{(\Phi I + A_{\max})^2 - 4\theta\Phi A_{\max} I}}{2\theta} - R_D, \quad (2)$$

where A is the net photosynthesis rate ($\mu\text{mol CO}_2 \cdot \text{m}^{-2} \cdot \text{s}^{-1}$), Φ is the initial slope of the curve ($\mu\text{mol CO}_2 \mu\text{mol}^{-1} \text{ PAR}$), A_{\max} is the maximum rate of photosynthesis ($\mu\text{mol CO}_2 \cdot \text{m}^{-2} \cdot \text{s}^{-1}$), I is the irradiance ($\mu\text{mol} \cdot \text{m}^{-2} \cdot \text{s}^{-1}$) of PAR, θ is a curvature parameter (dimensionless), and R_D is the respiration rate ($\mu\text{mol CO}_2 \cdot \text{m}^{-2} \cdot \text{s}^{-1}$). The calibration method is based on Cernusak et al. (2011). Values of Φ and R_D were fitted first by the least square method at I below $50 \mu\text{mol} \cdot \text{m}^{-2} \cdot \text{s}^{-1}$, and then A_{\max} and θ were estimated by the least square method. As the photosynthetic rates were measured at leaf scale but transpiration rates at the canopy scale, L_c was introduced to convert A_{\max} from leaf scale to canopy scale, and the maximum canopy photosynthetic rate was calculated by $A_{\max} L_c$. This is based on the model proposed by Bazzaz and Harper (1977) and on the assumption that the measured leaves represent the average of all leaves, in terms of leaf age, leaf distribution, nitrogen content, and so on. $L_c \pi$ ($\pi = 3.14$) was adopted for *A. verticillata* to convert A_{\max} from leaf scale to canopy scale. The inferred values of A_{\max} , Φ , θ , and R_D are shown in Table 2.

2.5 | The BTA transpiration model

The BTA model is formulated as

$$E_c = \frac{E_{\max}(R_s + R_0)D}{k + bR_s + (R_s + R_0)D}, \quad (3)$$

where E_c stands for canopy transpiration and E_{\max} is the maximum transpiration under optimal environmental conditions and can be fitted as a parameter. R_s means solar radiation (W m^{-2}), and D is the leaf to air vapour pressure deficit and can be approximated by air

TABLE 2 Parameters of photosynthetic light response curves (A_{\max} , Φ , θ , and R_D) measured by gas exchange

Species	A_{\max} ($\mu\text{mol CO}_2\cdot\text{m}^{-2}\cdot\text{s}^{-1}$)	Φ ($\mu\text{mol CO}_2 \mu\text{mol}^{-1}$ PAR)	θ (unitless)	R_D ($\mu\text{mol CO}_2\cdot\text{m}^{-2}\cdot\text{s}^{-1}$)
<i>Allocasuarina verticillata</i>	3.76	0.028	0.535	0.93
<i>Osmmanthus fragrans</i>	4.76	0.035	0.707	0.86
<i>Cinnamomum camphora</i>	13.94	0.055	0.308	2.22
<i>Liquidambar formosana</i>	8.41	0.048	0.554	1.76

Note. PAR: photosynthetically active radiation.

vapour pressure deficit (VPD) when canopy is coupled aerodynamically (Jarvis & McNaughton, 1986). We use VPD (kPa) as a surrogate for D in this study as we lacked estimates of canopy temperature. The parameters k ($\text{kPa}\cdot\text{W}\cdot\text{m}^{-2}$), b (kPa), and R_0 (W m^{-2}) are fitted. R_0 is included to enable the model to simulate nocturnal transpiration/sap flow ($R_0 > 0$ permits nonzero E_c at night, when $R_s = 0$). R_0 is set to zero when the model is used to simulate daily total transpiration.

2.6 | The BTA- ψ transpiration model

Darcy's Law was used to describe the relationship between canopy conductance (g_c), D , soil water potential, and the hydraulic conductance of the soil to leaf pathway (K_l) for fluid flow (Tyree & Ewers, 1991). If boundary layer conductance is large relative to g_c , then g_c is equal to $K_l (\psi_{\text{soil}} - \psi_{\text{leaf}})/D$ (e.g., Hubbard, Ryan, Stiller, & Sperry, 2001), where ψ_{leaf} is leaf water potential. For canopy well coupled with surrounding air, transpiration is controlled by canopy conductance (g_c) and vapour pressure deficit. Transpiration rates can be calculated as $E_c = g_c D$ (Whitehead, 1998; Whitley et al., 2009). Given that ψ_{leaf} cannot be more negative than $\psi_{s,\text{leaf}}$ (because $\psi_{\text{leaf}} = P_{\text{leaf}} + \psi_{s,\text{leaf}}$, and $P_{\text{leaf}} \geq 0$ [where P_{leaf} is leaf turgor pressure]), it follows that the gradient driving water flow to the canopy ($\psi_{\text{soil}} - \psi_{\text{leaf}}$) cannot be greater than $\psi_{\text{soil}} - \psi_{s,\text{leaf}}$, and hence, E_c cannot exceed a maximum value, E_{\max} , given by

$$E_{\max} = K_l (\psi_{\text{soil}} - \psi_{s,\text{leaf}}), \quad (4)$$

where K_l ($\text{mm}\cdot\text{MPa}^{-1}\cdot\text{hr}^{-1}$ or $\text{mm}\cdot\text{MPa}^{-1}\cdot\text{day}^{-1}$) is the stand-level hydraulic conductance and $\psi_{s,\text{leaf}}$ (MPa) is the solute potential (osmotic potential) of the leaf. The original model of Buckley et al. (2003) upon which BTA is based assumes $\psi_{s,\text{leaf}}$ to be more specifically that of the epidermis, but recent studies (Díaz-Espejo et al., 2012; Rodríguez-Domínguez et al., 2016) suggest that it represents bulk leaf osmotic potential. When measurements of soil water potential are available, the performance of the BTA model under water shortage can be improved by inserting Equation (4) into Equation (3), resulting in what we refer to as the BTA- ψ model:

$$E_c = \frac{K_l (\psi_{\text{soil}} - \psi_{s,\text{leaf}}) R_s D}{k + b R_s + R_s D} \quad (5)$$

at a daily scale, or

$$E_c = \frac{K_l (\psi_{\text{soil}} - \psi_{s,\text{leaf}}) (R_s + R_0) D}{k + b R_s + (R_s + R_0) D} \quad (6)$$

at an hourly scale (R_0 is included in Equation 6 to permit hourly variations in nocturnal transpiration to be simulated). Here, both K_l and $\psi_{s,\text{leaf}}$ are treated as fitted parameters, although we note that they have physiological meanings and can be measured experimentally (e.g., as shown by Rodríguez-Domínguez et al., 2016).

2.7 | Model calibration and parameter optimization

As rainfall may reduce the reliability of sap flow measurements and some measurements of predawn stem water potential were missing on rainy days, data from rainy days were not included in the analysis. To obtain a single parameterization for each species, we combined all types of data to train and test the BTA and BTA- ψ models by cross-validation, for both hourly and daily time steps. One half of the combined data (the "training" data) was randomly selected and used to calibrate the models, and the remaining half of the data (the "testing" data) was used to test the calibrated models. Results are presented only using the testing data.

In this study, we used the Differential Evolution Adaptive Metropolis (DREAM) algorithm (Vrugt, Braak, Clark, Hyman, & Robinson, 2008) to optimize parameter fitting for each model. DREAM requires users to input a distribution for the values of each parameter and to set the number of iterations. We estimated reasonable ranges for each parameter as follows. E_{\max} was set as the maximum value of all measured transpiration rates in the training period, and k , b , R_s , and K_l were allowed to range between 10 and 500 $\text{kPa}\cdot\text{W}\cdot\text{m}^{-2}$, 0.1 and 10 kPa, 0 and 50 W m^{-2} , and 0 and 5 $\text{mm}\cdot\text{MPa}^{-1}\cdot\text{hr}^{-1}$ or $\text{mm}\cdot\text{MPa}^{-1}\cdot\text{day}^{-1}$, respectively, based on the physical meaning of each parameter as well as the ranges identified automatically by the DREAM algorithm. Figure 2b indicates that the measured stem water potential of *A. verticillata* was lower than -5 MPa during drought. Thus, the range for $\psi_{s,\text{leaf}}$ was set to -10 to 0 MPa for *A. verticillata* and -5 to 0 MPa for *O. fragrans*, *C. camphora*, and *L. formosana*, which grow in a humid climate zone. DREAM runs 10 Markov chains at the same time and automatically searches the scale and orientation of the proposed parameter distributions using differential evolution. DREAM then produces 1,000 sets of parameters and calculates a score for each parameter set. Finally, DREAM outputs the numerical values of parameters with the best score.

2.8 | Model evaluation and validation

In order to quantify the predictive power of both models, two performance statistical indices, root mean square error (RMSE) and the

Nash–Sutcliffe coefficient of efficiency (NSE; Legates & McCabe, 1999; Nash & Sutcliffe, 1970), were used to evaluate the fitted models. RMSE is an effective measure of the deviation of model estimates from observed data. NSE indicates how well the predicted and observed values fit the 1:1 line, and it ranges between $-\infty$ and 1. Higher values of NSE indicate that the model simulation is in better agreement with the experimental observation, with NSE = 1 being optimal. If $\text{NSE} \geq 0.5$, the simulation can be considered satisfactory; if $\text{NSE} \geq 0.65$, the model is considered to perform well (Moriassi et al., 2007).

The Bayesian information criterion (BIC; Schwarz, 1978) penalizes inclusion of extra parameters in a model (Hawkins, 2003) to prevent overfitting. BIC is calculated as

$$\text{BIC} = n \log \left(\frac{\text{SSE}}{n} \right) + m \log(n), \quad (7)$$

where SSE is the sum of squared errors, n is the number of data points, and m is the number of predictors. A model is preferred if its BIC is smaller than others (Guan, Zhang, Makhnin, & Sun, 2013).

2.9 | Assessment of the physical processes from the model parameters

The sensitivity of transpiration to environmental drivers may vary across species (Whitley et al., 2013), and these differences can be reflected in the value of parameters for transpiration models such as BTA and BTA- ψ . In the BTA model, k and b are lumped parameters, given as (Buckley et al., 2012):

$$k = K_I / (\chi \phi), \quad (8)$$

$$b = K_I / (\chi \alpha_{\max}), \quad (9)$$

where K_I is the same as in Equation (4), χ ($\text{mm} \cdot \text{MPa}^{-1} \cdot \text{kPa}^{-1}$) is a factor that scales guard and epidermal cell turgor pressures to stomatal conductance and includes the effect of stomatal density, ϕ ($(\text{W m}^{-2})^{-1}$) is the initial slope of the response of guard cell advantage to irradiance, and α_{\max} (unitless) is the guard cell advantage at saturating irradiance. (The “guard cell advantage,” α , is a term from the original BMF model of Buckley et al., 2003, the premise of which is that guard cells actively adjust their osmotic pressures [π_g] in proportion to leaf turgor pressure [P_{leaf}]; α is the sensitivity of π_g to P_{leaf} , i.e., $\alpha = \partial \pi_g / \partial P_{\text{leaf}}$.) It is more convenient to consider the ratio of k/b rather than to analyse each single parameter, as the ratio eliminates χ and K_I , giving α_{\max} / ϕ , which only involves the solar radiation response components. A large k/b (i.e., α_{\max} / ϕ) means a large value of α_{\max} or small value of ϕ , or both. The values of α_{\max} / ϕ related to independent leaf-level gas exchange measurements. It is reasonable to analyse the results of k/b at hourly scale to compare with the value of $A_{\max} L_c / \Phi$ calculated by gas exchange data, which is measured instantaneously.

To quantify uncertainty in fitted parameters, we compared parameter values obtained using 20 different training datasets of varying sizes (25%, 50%, and 75% of all hourly data points) and reported the coefficient of variation (CV) for each value across training datasets;

CV quantifies the relative uncertainty in parameter ($\text{CV} = \text{standard deviation}/\text{mean}$). Ideally, final optimized parameters should have uncertainty smaller than that resulting from 20 training iterations based on 75% data.

3 | RESULTS

3.1 | Daily transpiration modelling

Statistical results of comparison between simulated daily transpiration rates and those derived from observed sap flow are shown in Figure 3. Figure 4 shows time series of simulations from both models and observations derived from sap flow for each target species at daily scale. Under conditions of sufficient soil moisture, both models performed comparably (e.g., in 2014 and 2015 for *C. camphora* and *L. formosana*), with differences below 0.02 in both RMSE (mm day^{-1}) and NSE (Figure 4c,d, respectively), indicating that the input of water potential to the BTA- ψ model is not necessary under sufficient water conditions.

However, the BTA model loses the ability to estimate transpiration rate when soil water potential varies widely, especially for *A. verticillata*, with NSE less than zero. In such conditions, BTA- ψ outperformed BTA significantly. For example, in *A. verticillata*, NSE = 0.602 for BTA- ψ versus -0.147 for BTA, and in *O. fragrans*, NSE = 0.590 for BTA- ψ versus 0.140 for BTA. The measured transpiration rates of two *O. fragrans* trees decreased gradually from July to August 2013 (~DOY 180 to 230) during a month-long drought, and the BTA model failed to capture this trend.

3.2 | Hourly transpiration modelling

Hourly transpiration rates were simulated for the entire measured period, and the statistical indicators of model performance are summarized in Figure 5. For *L. formosana*, NSE and BIC were comparable for both models. However, although the BTA model also performed well for *O. fragrans*, *C. camphora*, and *L. formosana*, with $\text{NSE} > 0.65$, the BTA- ψ model had much higher NSE and lower BIC in each species (although these differences were quite small for *L. formosana*). For example, for *A. verticillata*, NSE was 0.857 (BTA- ψ) versus 0.572 (BTA), for *O. fragrans*, NSE was 0.905 (BTA- ψ) versus 0.760 (BTA), and for *C. camphora*, NSE was 0.767 (BTA- ψ) versus 0.660 (BTA). The better performance of the BTA- ψ model is clearly evident in comparisons of hourly scale simulations and measurements during drought periods (Figure 6). The BTA model failed to capture wide variations in daily maximum transpiration rate during drought, with marked overestimation of midday transpiration. With the effect of soil water potential included, the simulations by the BTA- ψ model were in good agreement with observations during both daytime and night-time. These results indicate that BTA- ψ significantly improves transpiration simulation of these species under a wide range of water conditions at the hourly scale in both subtropical humid and Mediterranean climate zones.

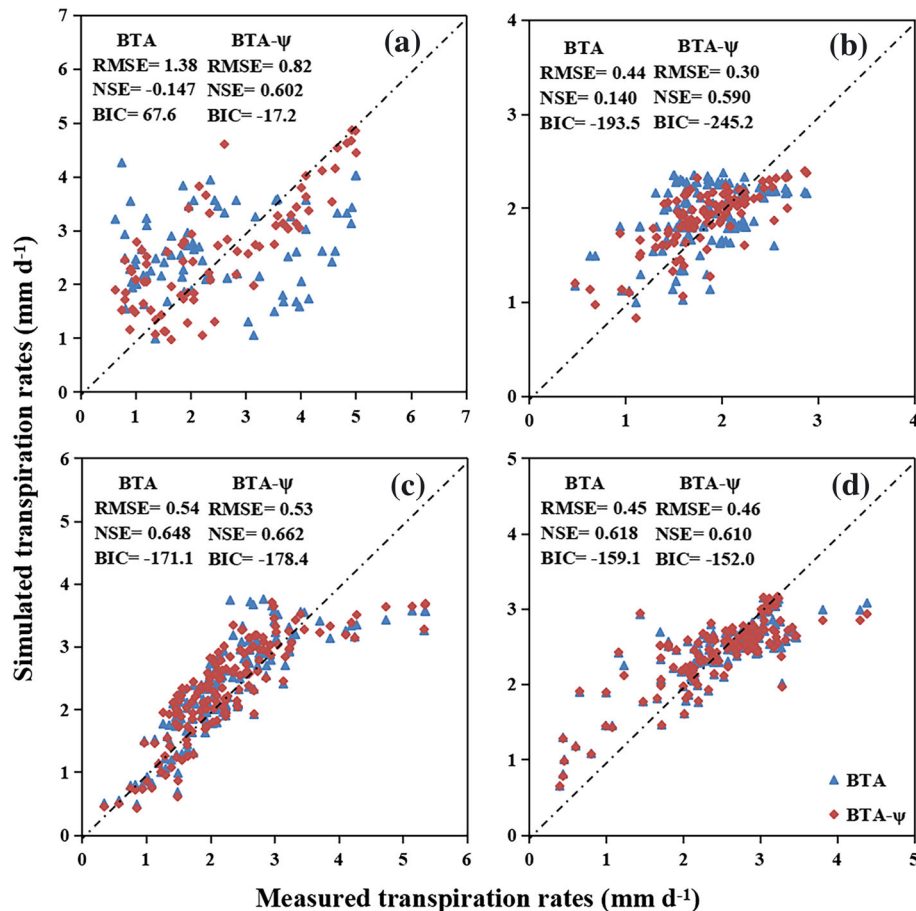


FIGURE 3 Calculated and simulated transpiration (E_c) for *Allocasuarina verticillata* (a), *Osmmanthus fragrans* (b), *Cinnamomum camphora* (c), and *Liquidambar formosana* (d) from the BTA and BTA- ψ models. The dot-dashed lines are 1:1 lines. BIC: Bayesian information criterion; NSE: Nash-Sutcliffe coefficient of efficiency; RMSE: root mean square error

3.3 | Nocturnal sap flow modelling

Both the BTA and BTA- ψ models accurately simulated nocturnal sap flow, within $\pm 10\%$, in the subtropical climate zone (Figure 7). However, the BTA- ψ model outperformed the BTA model for all species, especially for *A. verticillata* (e.g., the BTA model underestimated nocturnal transpiration by 15.5% in this species, vs. 1.7% underestimation by the BTA- ψ model).

3.4 | Comparison of parameters estimated by leaf gas exchange versus by calibration of transpiration models

The parameters in both models have a basis in leaf physiology, so physiological traits could potentially be inferred by fitting these models to sap flow and environmental data. We tested this potential by comparing parameters estimated from both models (using 100% of transpiration data to train the models) with those calculated directly from leaf gas exchange measurements. On the basis of Figure 8, which shows that the uncertainty of the calibrated parameters k , b , k/b , and R_0 decreases gradually with the increase of the size of training data,

we estimate that the uncertainty for each fitted parameter is 5% of its mean fitted value. We estimated photosynthetic parameters by fitting Equation (2) to leaf-level gas exchange measurements (Figure 9a). The ratio of the parameters k and b in the BTA and BTA- ψ models should be proportional to the quantity $A_{\max} L_c/\Phi$ calculated from gas exchange data, and our data generally support this prediction, with correlation coefficients of 0.84 for the BTA- ψ model and 0.70 for the BTA model (Figure 9b). This supports the notion that the parameters in the BTA and BTA- ψ models have physiological significance.

4 | DISCUSSION

4.1 | Advantage of the BTA- ψ model for simulating transpiration over a range of moisture conditions

The effect of soil water potential on transpiration under drought stress has long been incorporated in the soil-plant-atmosphere models, although typically using empirical models to capture this effect (Federer, 1979). Our results show that simulations of transpiration/sap flow were substantially improved by expanding

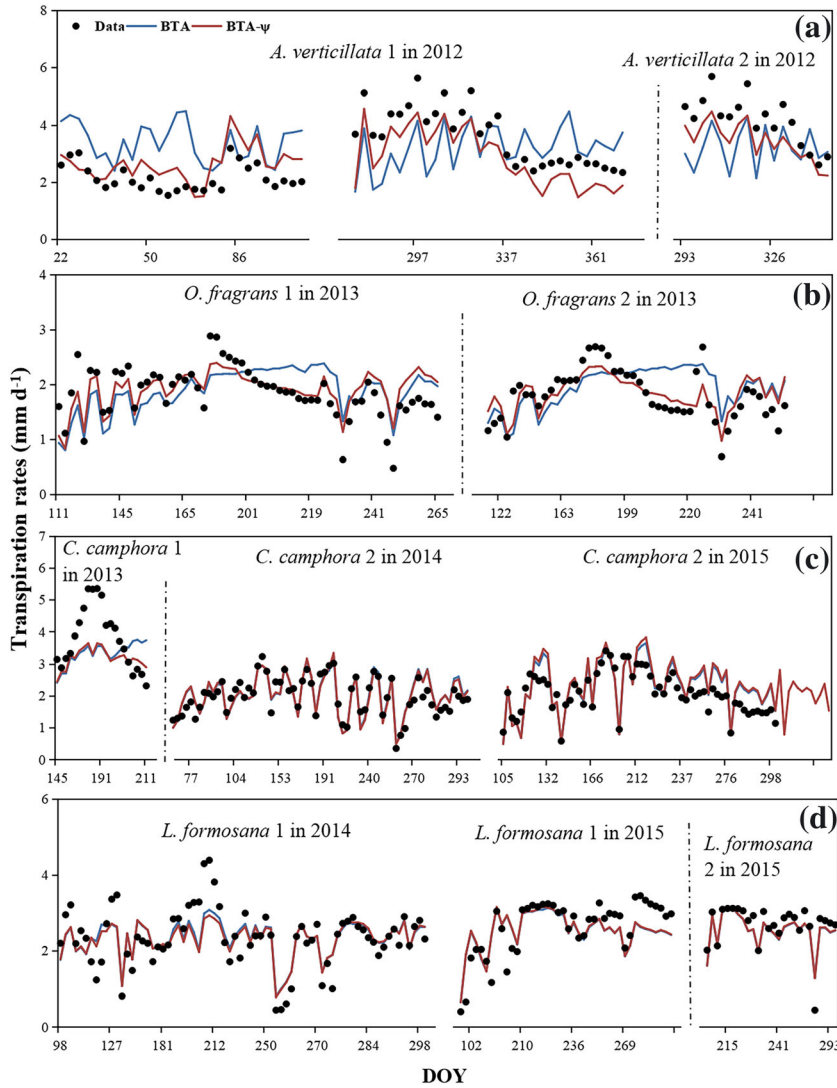


FIGURE 4 Simulated transpiration from the BTA and BTA- ψ models in comparison with the observations by sap flow measurement for *Allocasuarina verticillata* (a), *Osmmanthus fragrans* (b), *Cinnamomum camphora* (c), and *Liquidambar formosana* (d) at the daily scale

the parameter E_{\max} in the process-based BTA model to explicitly describe the effect of soil water potential, rather than treating E_{\max} as a constant during periods of varying soil moisture. These results demonstrate that a compact and tractable process-based model of canopy transpiration can be useful for predicting transpiration.

We found that the BTA and BTA- ψ models performed comparably under sufficient water conditions, but the BTA model failed in estimating transpiration when soil moisture varies widely. The results agree with the conclusions in Wang et al. (2016), in which BTA performed better within seasons than across seasons as soil moisture changed greatly, but contrast with results of Xu et al. (2017), who found that the BTA performed well over longer experiment periods (April to September in 2014 and 2015). Two possibilities may explain the different performances of the BTA model between these studies. The first is related to the different water sources between experimental sites. In Wang et al. (2016), stem water potential (MPa) tracked precipitation during summer, suggesting that precipitation is the primary (if not the only) source for root-zone soil water at that site. By contrast, Xu et al. (2017) performed measurements in a continental

arid temperate climate with hot and dry summers, on desert shrub species with deep root systems. Many ecosystems in arid and semi-arid regions are dependent on groundwater (Liu, Guan, Zhao, Yang, & Li, 2017). It is likely that the species in Xu et al. (2017) are groundwater dependent, in which case they would be relatively insensitive to fluctuations in moisture levels of the upper soil horizons caused by seasonal variation in precipitation. Indeed, Xu et al. (2017) noted that soil water content was significantly high below 20-cm depth. Another possibility is that the leaf osmotic potential ($\psi_{s,leaf}$) becomes more negative in magnitude in response to the root-zone soil water deficit in the species examined by Xu et al. (2017); such a pattern of “osmotic adjustment” is common (Turner, 2018) and helps to maintain active leaf gas exchange during soil drought. In the BTA model, osmotic adjustment would make the parameter E_{\max} relatively insensitive to soil drought, obviating the need to include ψ_{soil} explicitly in the model, as in the BTA- ψ model. Thus, we suggest that the BTA model can be used to estimate transpiration for species with reliable groundwater supply and/or strong osmotic adjustment, whereas the BTA- ψ model is more appropriate for species and sites that experience a wide range of soil water stress.

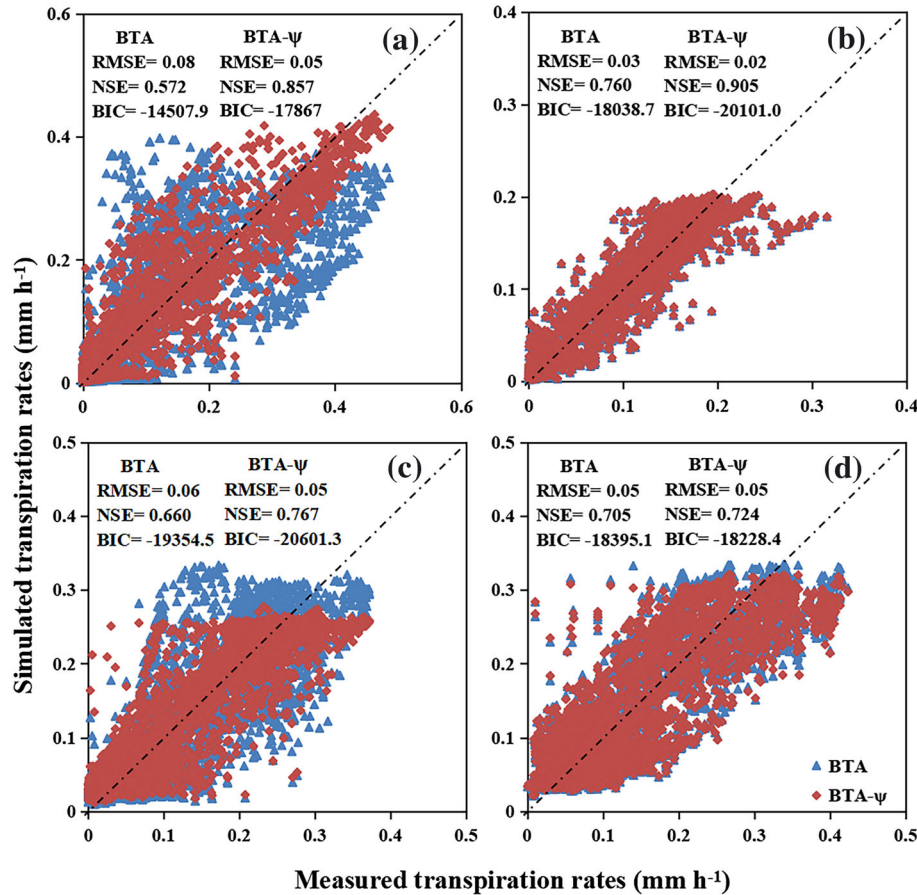


FIGURE 5 Hourly transpiration observed by sap flow and simulated by the BTA and BTA-ψ models, for *Allocasuarina verticillata* (a), *Osmmanthus fragrans* (b), *Cinnamomum camphora* (c), and *Liquidambar formosana* (d). The dot-dashed lines are 1:1 lines. BIC: Bayesian information criterion; NSE: Nash-Sutcliffe coefficient of efficiency; RMSE: root mean square error

4.2 | Inference of physiological properties from calibrated parameters

The structure and parameters of the BTA and BTA-ψ models can be traced directly to physiological mechanisms and properties, and thus, fitted parameters from these models are expected to reflect physiological difference across species, at least qualitatively. This means that model projections can be progressively improved as physiological understanding of the underlying processes improves. It also offers the prospect of using the model to understand the physiological basis of species differences in transpiration. For example, the ratio of the fitted parameters k and b , as well as the measured parameter combination $A_{\max} L_c / \Phi$ ($A_{\max} L_c \pi / \Phi$ for conifer species), which theory suggests should be proportional to k/b (Buckley et al., 2012), was greatest for *A. verticillata* among four species. This may reflect the greater total leaf surface area of the conifer *A. verticillata* and is consistent with the finding that maximum mean diurnal gross primary production is larger for temperate conifers than temperate broad-leaf deciduous trees (Falge et al., 2002). By contrast, k/b was lowest for *L. formosana*, which implies a large initial slope of the response of stomatal conductance to irradiance (ϕ ; Equation 8) and corresponds well with the large initial slope of the response of photosynthesis to irradiance (Φ) in this species. This is likely because *L. formosana* is a deciduous species with

current-year leaves, which are sensitive to radiation. Values of A_{\max} and Φ were greater in *C. camphora* than in *O. fragrans*, indicating that photosynthesis of *C. camphora* is more sensitive to light and reaches greater maximum rates. High photosynthetic rates in turn imply a large demand for water, which might explain why leaves of *C. camphora* senesced after a severe drought in 2013 whereas the *O. fragrans* canopy remained viable (Luo et al., 2016).

It should be noted that the fitted parameters from the BTA and BTA-ψ models differed in most cases. This difference is likely due to the fact that BTA cannot capture changes in soil moisture, due to the invariance of its parameter E_{\max} . This causes a compensatory shift in the model's other fitted parameters, leading them to deviate from their physical values. This problem was more pronounced for the three species that experienced varying soil moisture (*A. verticillata*, *O. fragrans*, and *C. camphora*), whereas fitted parameters for the BTA and BTA-ψ models agreed better for *L. formosana*, which was measured under well-watered conditions. The divergence between parameters fitted for the BTA and BTA-ψ models in the other three species questions the assumption, implicit in treating E_{\max} as a constant, that osmotic adjustment counterbalances changes in soil water potential in these species.

Such a problem of unrealistic fitted parameters in the BTA model can be found in published studies. For example, negative calibrated values

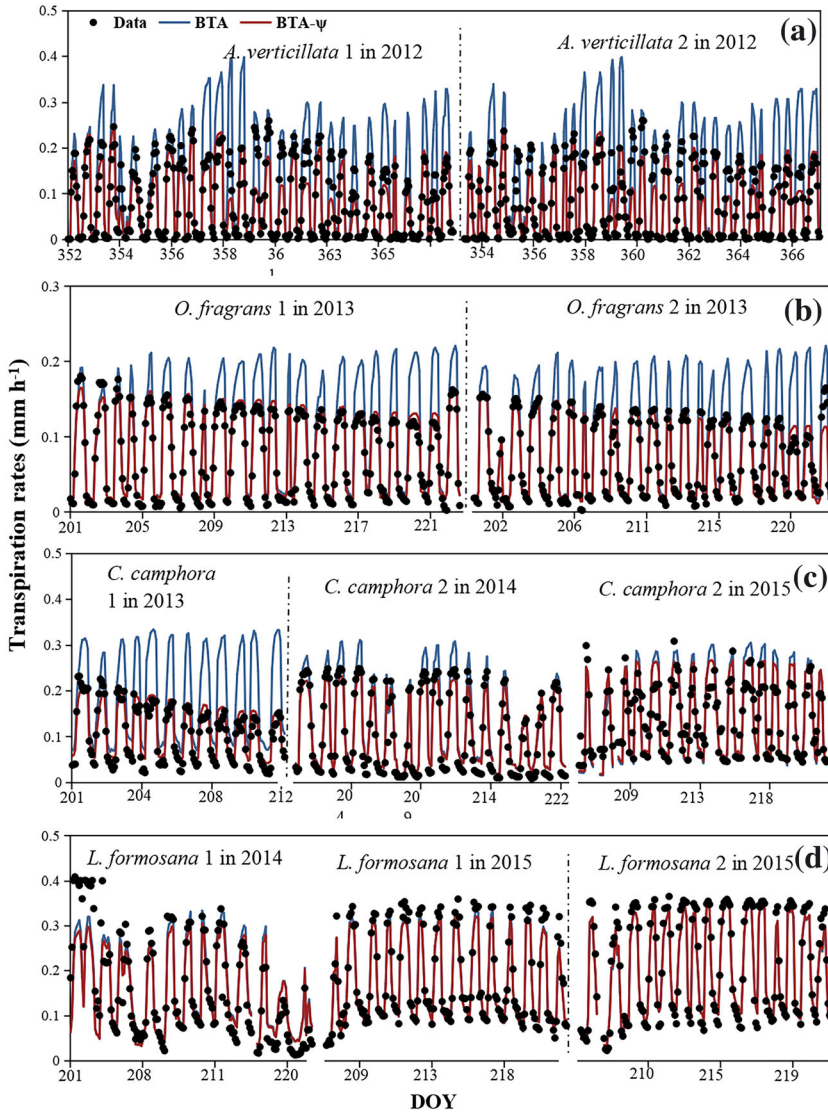


FIGURE 6 Simulated transpiration from the BTA and BTA- ψ models at the hourly scale in comparison with the observations under conditions of reduced soil moisture. Only data points for *Allocasuarina verticillata* (a) from December 15 to 31, 2012, and for *Osmanthus fragrans* (b), *Cinnamomum camphora* (c), and *Liquidambar formosana* (d) from July 20 to August 10 in each year from 2013 to 2015 are shown to have a better view for analysing the performance of models, as the dry season often occurs from the middle of July to the beginning of August in Changsha and a drought period is in December in Adelaide

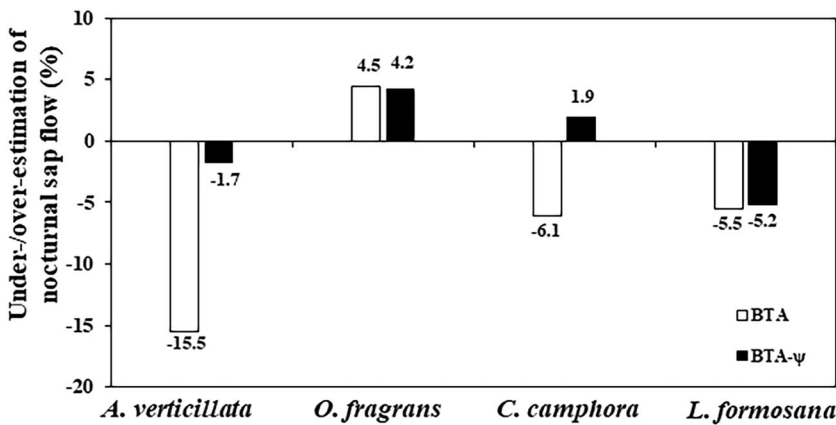


FIGURE 7 Comparison between nocturnal sap flow summed from each hourly simulation and sap flow measurements of each target species. The number above or below the bars is the overestimated or underestimated percentage by the BTA (open symbol) and BTA- ψ (solid symbol) models

have been reported for the parameter b (Buckley et al., 2012; Xu et al., 2017), which is not consistent with its physiological meaning. By contrast, fitted values of k/b in the BTA- ψ model are consistent with measured values of $A_{max} L_c/\Phi$. We suggest that caution is required in

inferring physiological parameters from calibrated parameters in individual species and that further study is necessary to resolve this. We also suggest that to obtain reasonable results, a reasonable initial range of parameters should be given based on the physiological backgrounds.

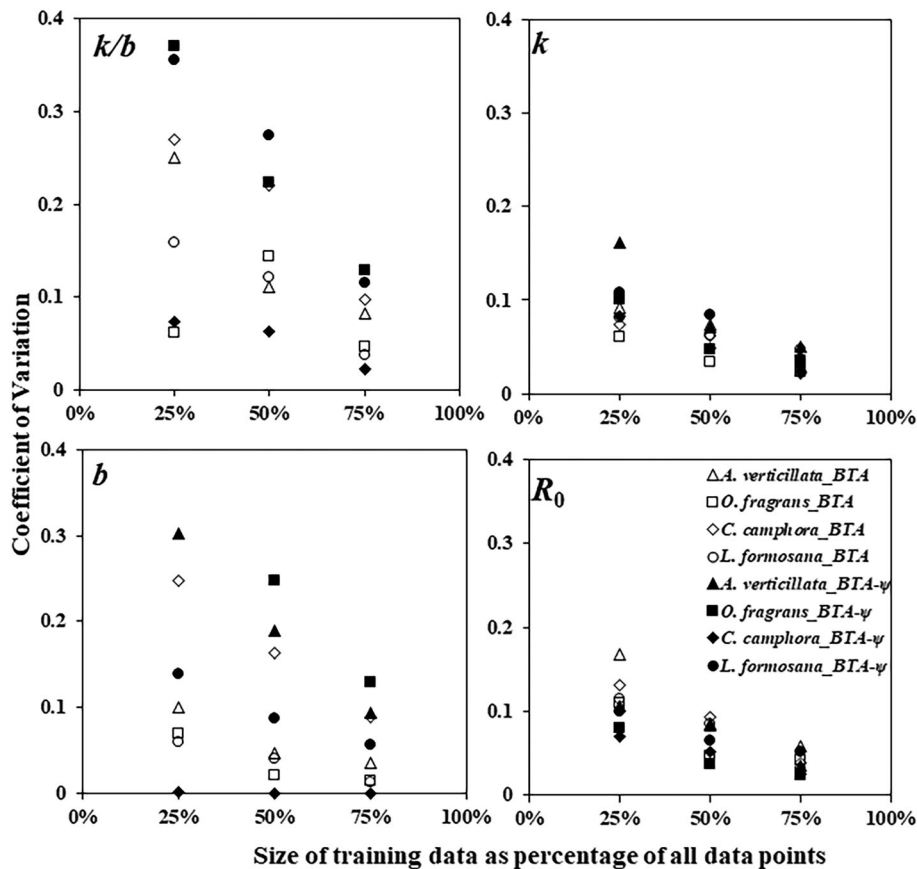


FIGURE 8 The coefficient of variation of the fitted parameters k , b , and R_0 in the BTA model (open symbols) and the BTA- ψ model (solid symbols), and the ratio k/b , obtained from 20 calibrations using various sizes of training datasets that are composed of 25%, 50%, and 75% of all hourly data points for four target species

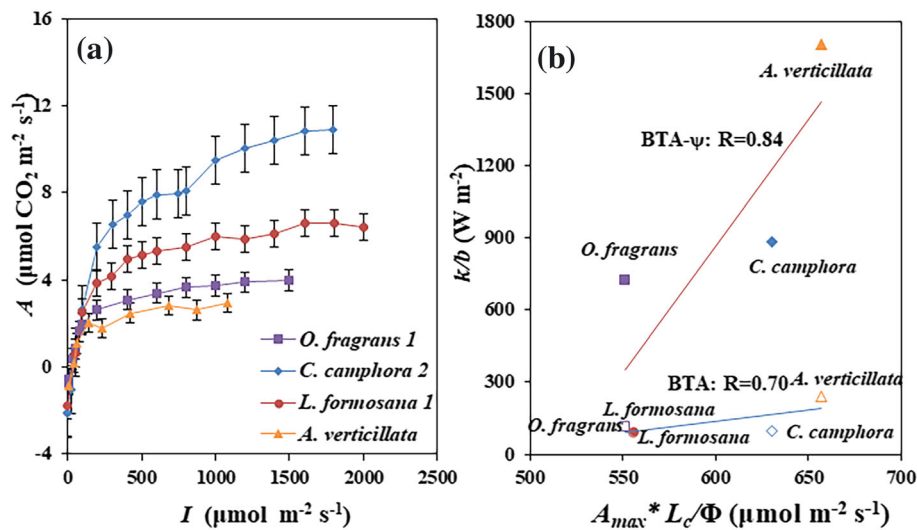


FIGURE 9 (a) Light response curves averaged for four *Allocasuarina verticillata* trees in 2017, *Osmmanthus fragrans* 1 in 2013, *Cinnamomum camphora* 2, and *Liquidambar formosana* 1 in 2015. Data of the species in Adelaide and in Changsha were collected in summer. (b) The relationship between $A_{max} L_c / \Phi$, calculated from observed leaf-level gas exchange, and k/b fitted for the BTA model (open symbols) and the BTA- ψ model (solid symbols) by cross-validation against whole-tree sap flow measurements

In addition, the fitted parameters based on hourly and daily data are significantly different for both BTA and BTA- ψ (Table 3). Similar results have been reported in previous studies with BTA (Buckley

et al., 2012; Wang et al., 2016; Xu et al., 2017). This result further confirms that parameters should be calibrated separately at different temporal scales (Wang et al., 2016).

TABLE 3 Parameter values for the BTA and BTA- ψ models calibrated using all data ("training data" + "testing data") by Differential Evolution Adaptive Metropolis at daily and hourly time scales

Model	Time scale	Species	k (kPa·W·m ⁻²)	b (kPa)	K_i (mm·MPa ⁻¹ ·hr ⁻¹ or mm·MPa ⁻¹ ·day ⁻¹)	$\psi_{s,leaf}$ (MPa)	R_0 (W m ⁻²)
BTA	Daily	<i>Allocasuarina verticillata</i>	66.5	1.01			
		<i>Osmmanthus fragrans</i>	15.7	0.59			
		<i>Cinnamomum camphora</i>	200.4	0.11			
		<i>Liquidambar formosana</i>	39.2	0.44			
	Hourly	<i>A. verticillata</i>	309.6	1.28			11.7
		<i>O. fragrans</i>	214.4	1.89			7.99
		<i>C. camphora</i>	112.5	1.15			15.4
		<i>L. formosana</i>	75.4	0.83			22.4
BTA- ψ	Daily	<i>A. verticillata</i>	96.6	0.10	1.05	-6.02	
		<i>O. fragrans</i>	10.3	0.64	0.69	-4.99	
		<i>C. camphora</i>	211.9	0.11	1.22	-4.99	
		<i>L. formosana</i>	29.2	0.32	0.82	-4.98	
	Hourly	<i>A. verticillata</i>	235.3	0.13	0.08	-6.18	15.9
		<i>O. fragrans</i>	146.3	0.20	0.05	-4.98	10.9
		<i>C. camphora</i>	88.5	0.10	0.09	-3.60	22.3
		<i>L. formosana</i>	68.3	0.71	0.10	-4.65	21.1

4.3 | Simulation of nocturnal sap flow

A particular strength of the BTA and BTA- ψ models, compared with other models (e.g., the MJS model), is their ability to estimate nocturnal transpiration or sap flow (Figure 7). Night-time transpiration has been observed across a range of ecosystems (e.g., Dawson et al., 2007; Novick, Oren, Stoy, Siqueira, & Katul, 2009; Snyder, Richards, & Donovan, 2003). Our data show substantial nocturnal sap flow for each of our study species, representing 6%, 7%, 14%, and 22% of total daily sap flow for *A. verticillata*, *O. fragrans*, *C. camphora*, and *L. formosana*, respectively. These values are within the range of reported night-time transpiration, for example, <10% for a range of desert shrubs (Xu et al., 2017), 6–10% for Australian native woody species (Buckley, Turnbull, Pfautsch, & Adams, 2011; Zeppel, Tissue, Taylor, Macinnis-Ng, & Eamus, 2010), and up to 40% for some Amazonian woody plants (Oliveira, Dawson, Burgess, & Nepstad, 2005). Because of the large magnitude of nocturnal water loss, it is important for models of evapotranspiration to include this phenomenon (e.g., Novick et al., 2009).

There have been some debates about whether nocturnal sap flow actually represents transpiration or instead represents flow of water into depleted water stores in tree trunks. The former interpretation is supported by the tight relationship typically reported between nocturnal sap flow and VPD, which drives transpiration (e.g., Buckley et al., 2011; Fisher, Baldocchi, Misson, Dawson, & Goldstein, 2007; Zeppel et al., 2010), and by the studies that used modelling to partition plant water recharge and transpiration (Buckley et al., 2011; Fisher et al., 2007). The BTA and BTA- ψ models cannot, by themselves, distinguish transpiration from storage flows. More direct validation of these models' nocturnal predictions would require either nocturnal measurements of stomatal conductance or sap flow measurements in branches, which are hydraulically distal to most of the trunk water storage volume.

4.4 | A common limitation of simplified transpiration models

A notable weakness of the BTA and BTA- ψ models is that neither model was able to capture the full range between the smallest and largest observed transpiration rates (e.g., Figures 4 and 6). Some simulated transpiration rates have a tendency towards an upper envelope as well as a lower bound, especially at hourly scale (Figure 5). The value of the upper bound is close to E_{max} (the maximum transpiration rate in the BTA model) and is limited by the fitted parameters K_i and $\psi_{s,leaf}$ in the BTA- ψ model. We found that the observed transpiration rates exceeded the fitted value of E_{max} because the latter was adjusted to optimize overall model fit, despite the fact that the quantities embedded within E_{max} (notably soil water potential) were in fact changing over the period for which the model was fitted. Because this is not consistent with the physical meaning of E_{max} , we decided to set E_{max} equal to the maximum observed value; however, this produces a negative bias, because in the BTA model, the transpiration rate can never actually reach E_{max} but can only approach it asymptotically (cf. Equation 3). The lower bound values are estimated at night and might be affected by these fitted parameters as well. A similar result was also found elsewhere using the MJS model (Macfarlane, White, & Adams, 2004; Wang et al., 2016; Whitley et al., 2013).

5 | CONCLUSIONS

The performance of the BTA model under conditions of varying soil moisture can be improved by incorporating the effect of root-zone soil water potential. For a species in Mediterranean climate zone and three species in subtropical humid zone at both daily and hourly scales, the BTA model's failure to predict transpiration accurately under water stress questions the assumption of osmotic adjustment that was

implicit in that model's treatment of the parameter E_{\max} as a constant. The improved model (BTA- ψ) is significantly better at predicting transpiration over a large range of moisture stress, although the BTA model was adequate under sufficient water conditions. Both models were able to predict nocturnal sap flow, though BTA- ψ was superior to BTA in this regard as well. Variation in calibrated parameters in both models corresponded reasonably well with measured variation in associated leaf-level physiological parameters.

The study provides modellers with an alternative transpiration model with simplified physiological representation and reasonable performance. Future work is required to test the improvements using new data from other bioclimatic zones and in larger scales, for example, based on eddy covariance flux measurements.

ACKNOWLEDGMENTS

This study was funded by the National Natural Science Foundation of China (Grants 41472238 and 41571021), National Centre for Groundwater Research and Training, Australia, Construct Program of Key Discipline in Hunan Province of China (Grant 2011001), Hunan Bairen Program (Grant 2012001), and Hunan Provincial Innovation Foundation for Postgraduate (Grant CX2017B181). N. L. and Z. D. L.'s contribution is partly supported by China Scholarship Council. T. N. B. acknowledges support from the National Science Foundation (Award 1557906), the International Wheat Yield Partnership (IWYP89, funded by the Grains Research and Development Corporation, US00082), and the USDA National Institute of Food and Agriculture, Hatch project 1016439.

ORCID

Na Liu  <https://orcid.org/0000-0003-1998-3978>

Xinguang He  <https://orcid.org/0000-0002-7570-3224>

Hailong Wang  <https://orcid.org/0000-0002-1091-0345>

Huade Guan  <https://orcid.org/0000-0001-5425-6974>

REFERENCES

- Allen, R.G., Pereira, L.S., Raes, D., & Smith, M. (1998). Crop evapotranspiration. Guidelines for computing crop water requirements. Irrigation and Drainage Paper no. 56. FAO, Rome.
- Bazzaz, F. A., & Harper, J. L. (1977). Demographic analysis of the growth of *Linum usitatissimum*. *New Phytologist*, 78(1), 193–208.
- Best, M. J., Pryor, M., Clark, D. B., Rooney, G. G., Essery, R. L. H., Ménard, C. B., ... Harding, R. J. (2011). The Joint UK Land Environment Simulator (JULES), model description—Part 1: Energy and water fluxes. *Geoscientific Model Development*, 4(3), 677–699. <https://doi.org/10.5194/gmd-4-677-2011>
- Beverly, C., Bari, M., Christy, B., Hocking, M., & Smettem, K. (2005). Predicted salinity impacts from land use change: Comparison between rapid assessment approaches and a detailed modelling framework. *Australian Journal of Experimental Agriculture*, 45(11), 1453–1469.
- Boussetta, S., Balsamo, G., Beljaars, A., Panareda, A. A., Calvet, J. C., Jacobs, C., ... van der Werf, G. (2013). Natural land carbon dioxide exchanges in the ECMWF integrated forecasting system: Implementation and offline validation. *Journal of Geophysical Research Atmospheres*, 118(12), 5923–5946. <https://doi.org/10.1002/jgrd.50488>
- Buckley, T. N., Mott, K. A., & Farquhar, G. D. (2003). A hydromechanical and biochemical model of stomatal conductance. *Plant, Cell & Environment*, 26(10), 1767–1785.
- Buckley, T. N., Turnbull, T. L., & Adams, M. A. (2012). Simple models for stomatal conductance derived from a process model: Cross-validation against sap flux data. *Plant, Cell & Environment*, 35(9), 1647–1662.
- Buckley, T. N., Turnbull, T. L., Pfautsch, S., & Adams, M. A. (2011). Nocturnal water loss in mature subalpine *Eucalyptus delegatensis* tall open forests and adjacent *E. pauciflora* woodlands. *Ecology and Evolution*, 1(3), 435–450.
- Burgess, S. S. O., Adams, M. A., Turner, N. C., Beverly, C. R., Ong, C. K., Khan, A. A. H., & Bleby, T. M. (2001). An improved heat pulse method to measure low and reverse rates of sap flow in woody plants. *Tree Physiology*, 21(9), 589–598.
- Cernusak, L. A., Hutley, L. B., Beringer, J., Jam, H., & Turner, B. L. (2011). Photosynthetic physiology of eucalypts along a sub-continental rainfall gradient in northern Australia. *Agricultural and Forest Meteorology*, 151(11), 1462–1470.
- Choudhury, B. J., & Digirolamo, N. E. (1998). A biophysical process-based estimate of global land surface evaporation using satellite and ancillary data I. Model description and comparison with observations. *Journal of Hydrology*, 205(3–4), 164–185.
- Cowan, I. R. (1982). Regulation of water use in relation to carbon gain in higher plants. *Encyclopedia of Plant Physiology*, 12, 589–613.
- Dawson, T. E., Burgess, S. S. O., Tu, K. P., Oliveira, R. S., Santiago, L. S., Fisher, J. B., ... Ambrose, A. R. (2007). Nighttime transpiration in woody plants from contrasting ecosystems. *Tree Physiology*, 27(4), 561–575.
- Diaz-Espejo, A., Buckley, T. N., Sperry, J. S., Cuevas, M. V., Cires, A. D., Elsayed-Farag, S., ... Fernandez, J. E. (2012). Steps toward an improvement in process-based models of water use by fruit trees: A case study in olive. *Agricultural Water Management*, 114(11), 37–49. <https://doi.org/10.1016/j.agwat.2012.06.027>
- Dickinson, R. E. (1987). Evapotranspiration in global climate models. *Advances in Space Research*, 7(11), 17–26.
- Dixon, M. A., & Tyree, M. T. (1984). A new stem hygrometer, corrected for temperature-gradients and calibrated against the pressure bomb. *Plant, Cell & Environment*, 7(9), 693–697.
- Falge, E., Baldocchi, D., Tenhunen, J., Aubinet, M., Bakwin, P., Berbigier, P., ... Wofsy, S. (2002). Seasonality of ecosystem respiration and gross primary production as derived from FLUXNET measurements. *Agricultural & Forest Meteorology*, 113(1), 53–74. [https://doi.org/10.1016/S0168-1923\(02\)00102-8](https://doi.org/10.1016/S0168-1923(02)00102-8)
- Fatichi, S., Pappas, C., & Ivanov, V. Y. (2016). Modeling plant-water interactions: An ecohydrological overview from the cell to the global scale. *WIREs. Water*, 3(3), 327–368. <https://doi.org/10.1002/wat2.1125>
- Federer, C. A. (1979). A soil-plant-atmosphere model for transpiration and availability of soil water. *Water Resources Research*, 15(3), 555–562. <https://doi.org/10.1029/WR015i003p00555>
- Feikema, P. M., Morris, J. D., Beverly, C. R., Collopy, J. J., Baker, T. G., & Lane, P. N. J. (2010). Validation of plantation transpiration in south-eastern Australia estimated using the 3PG+ forest growth model. *Forest Ecology and Management*, 260(5), 663–678. <https://doi.org/10.1016/j.foreco.2010.05.022>
- Fisher, J. B., Baldocchi, D. D., Misson, L., Dawson, T. E., & Goldstein, A. H. (2007). What the towers don't see at night: Nocturnal sap flow in trees and shrubs at two AmeriFlux sites in California. *Tree Physiology*, 27(4), 597–610. <https://doi.org/10.1093/treephys/27.4.597>
- Gao, Q., Zhao, P., Zeng, X., Cai, X., & Shen, W. (2002). A model of stomatal conductance to quantify the relationship between leaf transpiration,

- microclimate and soil water stress. *Plant, Cell & Environment*, 25(11), 1373–1381. <https://doi.org/10.1046/j.1365-3040.2002.00926.x>
- Gharbia, S. S., Smullen, T., Gill, L., Johnston, P., & Pilla, F. (2018). Spatially distributed potential evapotranspiration modeling and climate projections. *Science of the Total Environment*, 633, 571–592. <https://doi.org/10.1016/j.scitotenv.2018.03.208>
- Gharun, M., Turnbull, T. L., Henry, J., & Adams, M. A. (2015). Mapping spatial and temporal variation in tree water use with an elevation model and gridded temperature data. *Agricultural and Forest Meteorology*, 200(1), 249–257. <https://doi.org/10.1016/j.agrformet.2014.09.027>
- Guan, H., & Wilson, J. L. (2009). A hybrid dual-source model for potential evaporation and transpiration partitioning. *Journal of Hydrology*, 377(3), 405–416. <https://doi.org/10.1016/j.jhydrol.2009.08.037>
- Guan, H., Zhang, X., Makhnin, O., & Sun, Z. (2013). Mapping mean monthly temperatures over a coastal hilly area incorporating terrain aspect effects. *Journal of Hydrometeorology*, 14(1), 233–250. <https://doi.org/10.1175/JHM-D-12-014.1>
- Hartmann, H., Ziegler, W., Kolle, O., & Trumbore, S. (2013). Thirst beats hunger—declining hydration during drought prevents carbon starvation in Norway spruce saplings. *New Phytologist*, 200(2), 340–349. <https://doi.org/10.1111/nph.12331>
- Hawkins, D. M. (2003). The problem of overfitting. *Journal of chemical information and computer sciences*, 44(1), 1–12.
- Houghton, J. T., Jenkins, G. J., & Ephraums, J. J. (1990). *Climate change. The IPCC scientific assessment* (Vol. 365). London: Cambridge University Press.
- Hubbard, R. M., Ryan, M. G., Stiller, V. S., & Sperry, J. S. (2001). Stomatal conductance and photosynthesis vary linearly with plant hydraulic conductance in ponderosa pine. *Plant, Cell & Environment*, 24, 113–121.
- Jarvis, P. G. (1976). The interpretation of the variations in leaf water potential and stomatal conductance found in canopies in the field. *Philosophical Transactions of the Royal Society B*, 273(927), 593–610. <https://doi.org/10.1098/rstb.1976.0035>
- Jarvis, P. G., & McNaughton, K. G. (1986). Stomatal control of transpiration: Scaling up from leaf to region. *Advances in Ecological Research*, 15, 1–49. [https://doi.org/10.1016/S0065-2504\(08\)60119-1](https://doi.org/10.1016/S0065-2504(08)60119-1)
- Johnson, I. R., & Thornley, J. H. M. (1984). A model of instantaneous and daily canopy photosynthesis. *Journal of Theoretical Biology*, 107(4), 531–545. [https://doi.org/10.1016/S0022-5193\(84\)80131-9](https://doi.org/10.1016/S0022-5193(84)80131-9)
- Khamzina, A., Sommer, R., Jpa, L., & Plg, V. (2009). Transpiration and early growth of tree plantations established on degraded cropland over shallow saline groundwater table in northwest Uzbekistan. *Agricultural and Forest Meteorology*, 149(11), 1865–1874. <https://doi.org/10.1016/j.agrformet.2009.06.015>
- Legates, D. R., & McCabe, G. J. (1999). Evaluating the use of “goodness of fit” measures in hydrologic and hydroclimatic model validation. *Water Resources Research*, 35(1), 233–241. <https://doi.org/10.1029/1998WR900018>
- LeMone, M. A., Chen, F., Alfieri, J. G., Tewari, M., Geerts, B., Miao, Q., ... Coulter, R. L. (2007). Influence of land cover and soil moisture on the horizontal distribution of sensible and latent heat fluxes in southeast Kansas during IHOP_2002 and CASES-97. *Journal of Hydrometeorology*, 8(1), 68–87. <https://doi.org/10.1175/JHM554.1>
- Liu, B., Guan, H., Zhao, W., Yang, Y., & Li, S. (2017). Groundwater facilitated water-use efficiency along a gradient of groundwater depth in arid northwestern China. *Agricultural and Forest Meteorology*, 233, 235–241. <https://doi.org/10.1016/j.agrformet.2016.12.003>
- Liu, N., Guan, H., Luo, Z., Zhang, C., Wang, H., & Zhang, X. (2017). Examination of a coupled supply- and demand-induced stress function for root water uptake modeling. *Hydrology Research*, 48(1), 67–77.
- Luo, Z., Guan, H., Zhang, X., & Liu, N. (2017). Photosynthetic capacity of senescent leaves for a subtropical broadleaf deciduous tree species *Liquidambar formosana* Hance. *Scientific Reports*, 7(6323), 1–9.
- Luo, Z., Guan, H., Zhang, X., Zhang, C., Liu, N., & Li, G. (2016). Responses of plant water use to a severe summer drought for two subtropical tree species in the central southern China. *Journal of Hydrology: Regional Study*, 8, 1–9.
- Macfarlane, C., White, D. A., & Adams, M. A. (2004). The apparent feed-forward response to vapour pressure deficit of stomata in droughted, field-grown *Eucalyptus globulus* Labill. *Plant, Cell & Environment*, 27(10), 1268–1280. <https://doi.org/10.1111/j.1365-3040.2004.01234.x>
- Marshall, B., & Biscoe, P. V. (1980). A model for C₃ leaves describing the dependence of net photosynthesis on irradiance: II. Application to the analysis of flag leaf photosynthesis. *Journal of Experimental Botany*, 31(120), 41–48. <https://doi.org/10.1093/jxb/31.1.41>
- McDowell, N., Pockman, W. T., Allen, C. D., Breshears, D. D., Cobb, N., Kolb, T., ... Yezzer, E. A. (2008). Mechanisms of plant survival and mortality during drought: Why do some plants survive while others succumb to drought? *New Phytologist*, 178(4), 719–739. <https://doi.org/10.1111/j.1469-8137.2008.02436.x>
- Mission, L., Panek, J. A., & Goldstein, A. H. (2004). A comparison of three approaches to modeling leaf gas exchange in annually drought-stressed ponderosa pine forests. *Tree Physiology*, 24(5), 529–541. <https://doi.org/10.1093/treephys/24.5.529>
- Moriasi, D. N., Arnold, J. G., Liew, M. W. V., Bingner, R. L., Harmel, R. D., & Veith, T. L. (2007). Model evaluation guidelines for systematic quantification of accuracy in watershed simulations. *Transaction of ASABE*, 50(3), 885–900. <https://doi.org/10.13031/2013.23153>
- Nash, J. E., & Sutcliffe, J. V. (1970). River flow forecasting through conceptual models part I—A discussion of principles. *Journal of Hydrology*, 10(3), 282–290. [https://doi.org/10.1016/0022-1694\(70\)90255-6](https://doi.org/10.1016/0022-1694(70)90255-6)
- Novick, K. A., Oren, R., Stoy, P. C., Siqueira, M. B. S., & Katul, G. G. (2009). Nocturnal evapotranspiration in eddy-covariance records from three co-located ecosystems in the Southeastern U.S.: Implications for annual fluxes. *Agricultural and Forest Meteorology*, 149, 1491–1504. <https://doi.org/10.1016/j.agrformet.2009.04.005>
- Oki, T., & Kanae, S. (2006). Global hydrological cycles and world water resources. *Science*, 313(5790), 1068–1072. <https://doi.org/10.1126/science.1128845>
- Oleson, K. W., Lawrence, D. M., Bonan, G. B., Flanner, M. G., Kluzek, E., Lawrence, P. J., ... Zeng, X. (2010). *Technical description of version 4.0 of the Community Land Model (CLM)*. NCAR Technical Note NCAR/TN-478pSTR. Boulder, CO: National Center for Atmospheric Research. 257 pp
- Oliveira, R. S., Dawson, T. E., Burgess, S. S. O., & Nepstad, D. C. (2005). Hydraulic redistribution in three Amazonian trees. *Oecologia*, 145, 354–363. <https://doi.org/10.1007/s00442-005-0108-2>
- Pekin, B., & Macfarlane, C. (2009). Measurement of crown cover and leaf area index using digital cover photography and its application to remote sensing. *Remote Sensing*, 1(4), 4335–4346.
- Pereira, A. R., Green, S., & Nova, N. A. V. (2006). Penman–Monteith reference evapotranspiration adapted to estimate irrigated tree transpiration. *Agricultural Water Management*, 83(1), 153–161. <https://doi.org/10.1016/j.agwat.2005.11.004>
- Rodríguez-Dominguez, C. M., Buckley, T. N., Egea, G., Cires, A., Hernandez-Santana, V., Martorell, S., & Diaz-Espejo, A. (2016). Most stomatal closure in woody species under moderate drought can be explained by stomatal responses to leaf turgor. *Plant, Cell & Environment*, 39(9), 2014–2026. <https://doi.org/10.1111/pce.12774>

- Saccon, P. (2018). Water for agriculture, irrigation management. *Applied soil ecology*, 123, 793–796. <https://doi.org/10.1016/j.apsoil.2017.10.037>
- Schlesinger, W. H., & Jasechko, S. (2014). Transpiration in the global water cycle. *Agricultural and Forest Meteorology*, 189–190(6), 115–117. <https://doi.org/10.1016/j.agrformet.2014.01.011>
- Schwarz, G. E. (1978). Estimating the dimension of a model. *Annals of Statistics*, 6(2), 461–464. <https://doi.org/10.1214/aos/1176344136>
- Snyder, K. A., Richards, J. H., & Donovan, L. A. (2003). Night-time conductance in C-3 and C-4 species: Do plants lose water at night? *Journal of Experimental Botany*, 54, 861–865. <https://doi.org/10.1093/jxb/erg082>
- Stewart, J. B. (1988). Modeling surface conductance of pine forest. *Agricultural and Forest Meteorology*, 43(1), 19–35. [https://doi.org/10.1016/0168-1923\(88\)90003-2](https://doi.org/10.1016/0168-1923(88)90003-2)
- Turner, N. C. (2018). Turgor maintenance by osmotic adjustment: 40 years of progress. *Journal of Experimental Botany*, 69(3), 3223–3233. <https://doi.org/10.1093/jxb/ery181>
- Tyree, M. T., & Ewers, F. W. (1991). Tansley Review no. 34. The hydraulic architecture of trees and other woody plants. *New Phytologist*, 119, 345–360. <https://doi.org/10.1111/j.1469-8137.1991.tb00035.x>
- Vrugt, J. A., Braak, C. J. F. T., Clark, M. P., Hyman, J. M., & Robinson, B. A. (2008). Treatment of input uncertainty in hydrologic modeling: Doing hydrology backward with Markov chain Monte Carlo simulation. *Water Resources Research*, 44(12), 5121–5127.
- Wang, H., Guan, H., Deng, Z., & Simmons, C. T. (2014). Optimization of canopy conductance models from concurrent measurements of sap flow and stem water potential on drooping sheoak in South Australia. *Water Resources Research*, 50, 6154–6167.
- Wang, H., Guan, H., & Simmons, C. T. (2016). Modeling the environmental controls on tree water use at different temporal scales. *Agricultural and Forest Meteorology*, 225, 24–35. <https://doi.org/10.1016/j.agrformet.2016.04.016>
- Wei, H., Xia, Y., Mitchell, K. E., & Ek, M. B. (2013). Improvement of the Noah land surface model for warm season processes: Evaluation of water and energy flux simulation. *Hydrological Processes*, 27(2), 297–303. <https://doi.org/10.1002/hyp.9214>
- White, D. A., Beadle, C. L., Sands, P. J., Worledge, D., & Honeysett, J. L. (1999). Quantifying the effect of cumulative water stress on stomatal conductance of *Eucalyptus globulus* and *Eucalyptus nitens*: A phenomenological approach. *Functional Plant Biology*, 26(1), 17–27. <https://doi.org/10.1071/PP98023>
- Whitehead, D. (1998). Regulation of stomatal conductance and transpiration in forest canopies. *Tree Physiology*, 18, 633–644. <https://doi.org/10.1093/treephys/18.8-9.633>
- Whitley, R., Medlyn, B., Zeppel, M., Macinnis-Ng, C., & Eamus, D. (2009). Comparing the Penman–Monteith equation and a modified Jarvis–Stewart model with an artificial neural network to estimate stand-scale transpiration and canopy conductance. *Journal of Hydrology*, 373(1), 256–266. <https://doi.org/10.1016/j.jhydrol.2009.04.036>
- Whitley, R., Taylor, D., Macinnis-Ng, C., Zeppel, M., Yunusa, I. A. M., O'Grady, A., ... Eamus, D. (2013). Developing an empirical model of canopy water flux describing the common response of transpiration to solar radiation and VPD across five contrasting woodlands and forests. *Hydrological Processes*, 27(8), 1133–1146. <https://doi.org/10.1002/hyp.9280>
- Xu, S., Yu, Z., Ji, X., & Studicky, E. A. (2017). Comparing three models to estimate transpiration of desert shrubs. *Journal of Hydrology*, 550, 603–615. <https://doi.org/10.1016/j.jhydrol.2017.05.027>
- Yang, Y., Guan, H., Hutson, J. L., Wang, H., Ewenz, C., Shang, S., & Simmons, C. T. (2013). Examination and parameterization of the root water uptake model from stem water potential and sap flow measurements. *Hydrological Processes*, 27(20), 2857–2863.
- Zeppel, M., Tissue, D., Taylor, D., Macinnis-Ng, C., & Eamus, D. (2010). Rates of nocturnal transpiration in two evergreen temperate woodland species with differing water-use strategies. *Tree Physiology*, 30(8), 988–1000. <https://doi.org/10.1093/treephys/tpq053>

How to cite this article: Liu N, Buckley TN, He X, et al. Improvement of a simplified process-based model for estimating transpiration under water-limited conditions. *Hydrological Processes*. 2019;33:1670–1685. <https://doi.org/10.1002/hyp.13430>